Published in final edited form as:
Anat Rec (Hoboken). 2010 November ; 293(11): 1971–1983. doi:10.1002/ar.21242.

Ontogeny of the Kidney and Renal Developmental Markers in the Rhesus Monkey (*Macaca mulatta*)

Cynthia A. Batchelder, PhD[1], **C. Chang I. Lee, PhD**[1], **Michele L. Martinez, MS**[1], and **Alice F. Tarantal, PhD**[1,2]

[1]Center of Excellence in Translational Human Stem Cell Research, California National Primate Research Center, School of Medicine, University of California, Davis, CA, 95616-8542, USA

[2]Departments of Pediatrics and Cell Biology and Human Anatomy, School of Medicine, University of California, Davis, CA, 95616-8542, USA

Abstract

Nonhuman primates share many developmental similarities with humans, thus they provide an important preclinical model for understanding the ontogeny of biomarkers of kidney development and assessing new cell-based therapies to treat human disease. To identify morphological and developmental changes in protein and RNA expression patterns during nephrogenesis, immunohistochemistry and quantitative real-time PCR were used to assess temporal and spatial expression of WT1, Pax2, Nestin, Synaptopodin, alpha-smooth muscle actin (α-SMA), CD31, vascular endothelial growth factor (VEGF), and Gremlin. Pax2 was expressed in the condensed mesenchyme surrounding the ureteric bud and in the early renal vesicle. WT1 and Nestin were diffusely expressed in the metanephric mesenchyme, and expression increased as the Pax2-positive condensed mesenchyme differentiated. The inner cleft of the tail of the S-shaped body contained the podocyte progenitors (visceral epithelium) that were shown to express Pax2, Nestin, and WT1 in the early second trimester. With maturation of the kidney, Pax2 expression diminished in these structures, but was retained in cells of the parietal epithelium, and as WT1 expression was upregulated. Mature podocytes expressing WT1, Nestin, and Synaptopodin were observed from the mid-third trimester through adulthood. The developing glomerulus was positive for α-SMA (vascular smooth muscle) and Gremlin (mesangial cells), CD31 (glomerular endothelium), and VEGF (endothelium), and showed loss of expression of these markers as glomerular maturation was completed. These data form the basis for understanding nephrogenesis in the rhesus monkey and will be useful in translational studies that focus on embryonic stem and other progenitor cell populations for renal tissue engineering and repair.

Keywords

Kidney; Ontogeny; Nephrogenesis; Development; WT1; Pax2; Nestin; Progenitors

INTRODUCTION

Stem and progenitor cells hold the potential for new therapies for many chronic and debilitating illnesses (Nirmalanandhan and Sittampalam, 2009). When coupled with strategies for organ regeneration and repair, stem and progenitor cells may revolutionize treatments for a wide variety of diseases some of which can be diagnosed prenatally

Author for correspondence: Alice F. Tarantal, PhD California National Primate Research Center Pedrick and Hutchison Roads University of California, Davis, California 95616-8542, USA Phone #: 530-752-6680, Fax #: 530-752-2880 aftarantal@primate.ucdavis.edu.

(Tarantal et al., 2001; Rao and Palmer, 2009). Current treatment options for patients with end-stage renal failure include dialysis, which involves severe lifestyle restrictions, or kidney transplant with life-long immune suppression. Approximately 80% of all candidates in need of replacement organs are waiting for a kidney, and limited organ availability highlights the need to develop new strategies to treat these patients in need (Organ Procurement and Transplantation Network, 2008). Diabetes, hypertension, obesity, and cardiovascular disease can also have a negative impact on kidney function, and the increasing prevalence of these health problems suggests that the current shortage of available kidneys for transplant and the number of patients in need will continue to increase (Coresh et al., 2007).

A thorough understanding of human development is vital for identifying new methods to effectively differentiate, for example, human embryonic stem cells towards renal lineages with the goal of using these precursors for organ regeneration and repair (Batchelder et al., 2009). The identification of biomarkers and expression patterns important during ontogeny provide essential clues for discovery of critical cell populations that may be useful for therapeutic interventions. Animal models are essential to advance translational research and provide the *in vivo* testing necessary to determine safety of these approaches prior to clinical trials in humans. Nonhuman primates share many developmental similarities with humans and thus they are an important model to advance new therapies for the treatment of human diseases (Bontrop, 2001; Lee et al., 2001; Tarantal et al., 2001; Shively and Clarkson, 2009), and can address questions that cannot be answered in other species (Little and Rae, 2009; Mezquita et al., 2008).

The goals of the current study were to characterize kidney development in the rhesus monkey to further assess the relevance to human development (Matsell and Tarantal, 2002), and to provide a baseline for future studies focused on prenatal cell and gene-based therapies to correct congenital disorders of the kidney, such as obstructive renal disease (Tarantal et al., 2001; Matsell et al., 2002; Butt et al., 2007). These goals were accomplished by: (1) morphologic analyses at a range of prenatal and postnatal ages; and (2) assessments of protein (immunohistochemical) and gene expression (PCR) profiles for genes with dual roles in development and disease (e.g., Wilm's tumor, renal hypoplasia, fibrosis) including Wilm's tumor 1 (WT1) (Pritchard-Jones et al., 1991), paired box gene 2 (Pax2) (Dressler et al., 1990), the intermediate filament Nestin (Chen et al., 2006), the podocyte marker Synaptopodin (Mundel et al., 1991; 1997), alpha-smooth muscle actin (α-SMA) (MacPherson et al., 1993), and Gremlin, a bone morphogenetic protein antagonist and mesangial cell marker (McMahon et al., 2000).

MATERIALS AND METHODS

Animals

All animal procedures were approved prior to implementation by the Institutional Animal Care and Use Committee at the University of California, Davis, and were consistent with the requirements of the Animal Welfare Act. Activities related to animal care such as diet and housing were performed as per standard operating procedures at the California National Primate Research Center. Normally cycling, adult female rhesus monkeys with a history of prior pregnancy were bred and identified as pregnant according to established methods (Tarantal, 2005) to obtain fetal specimens (N=21). Fetal tissues were collected by hysterotomy using aseptic techniques and established protocols (Tarantal et al., 2001) during the first trimester (25 to 55 days gestation; N=7), second trimester (70 to 100 days gestation; N=7), and third trimester (110 days gestation to tem; N=7) (term 165±10 days). All dams were returned to the colony post-procedure. Postnatal (3-6 months; N=3) and adult (> 4 years; N=3) specimens previously collected were also included in the analysis. Tissues were

placed in 10% buffered formalin, embedded in paraffin, and sectioned at 5-6 μm for morphologic and immunohistochemical analyses, and cryopreserved sections were used for molecular assessments.

Immunohistochemistry

Immunohistochemistry was performed as previously described (Batchelder et al., 2009). Briefly, tissue sections were deparaffinized in xylene, rehydrated in a graded series of ethanol, and washed in phosphate-buffered saline (PBS). Antigen retrieval was accomplished with hot citrate buffer (pH 6.0) followed by gradual cooling and transfer to PBS according to the manufacturer's specifications (Decloaking Chamber, Biocare Medical, Concord, CA, USA). Sections were washed twice in PBS for 5 min each and incubated for 1 hr in blocking buffer with 2% serum of the secondary antibody host species. After brief washes in PBS (two washes, 2 min each), sections were incubated in primary antibody overnight at 4°C and PBS wash steps repeated prior to incubation for 1 hr with secondary antibody at room temperature in the dark. Primary antibodies included WT1 (Invitrogen, Carlsbad, CA, USA), Pax2 (Invitrogen), Nestin (Millipore, Billerica, MA, USA), Synaptopodin (Progen Biotechnik, Heidelberg, Germany), α-SMA (Millipore), CD 31 (Dako, Carpinteria, CA, USA), vascular endothelial growth factor (VEGF) (Millipore), and Gremlin (Abcam, Cambridge, MA, USA). Sections were then washed again in PBS twice and coverslips mounted with ProLong Gold® with Dapi (Invitrogen) and slides imaged with an Olympus BX61 fluorescent microscope equipped with a Photometrics CoolSnap HAQ black and white camera (Olympus, Center Valley PA, USA). Formalin-fixed sections were also analyzed morphologically by staining with hemotoxylin and eosin (H&E) using standard protocols.

Quantitative Real-time PCR

Tissue samples were collected in RNA*later*® RNA Stabilization Reagent (Qiagen, Valencia, CA, USA), snap frozen immediately in liquid nitrogen, and stored at ≤−80°C until processing. Total RNA was extracted following the manufacturer's instructions from 5-20 mg of tissue with the RNeasy Plus Mini Kit (Qiagen). cDNA was synthesized using random primers and the Sensiscript® Reverse Transcription Kit (Qiagen) according to the manufacturer's protocol. Primers for PCR (Table 1) were designed to span an exon junction and thus eliminate the possibility of amplifying genomic DNA templates remaining in the RNA preparations. Real-time PCR was carried out in duplicate in 96-well optical plates using the 7900® ABI Sequence Detection System (Applied Biosystems, Foster City, CA, USA) and the QuantiTect™ SYBR® Green PCR Kit (Qiagen) according to the manufacturer's protocols as previously described (Batchelder et al., 2009). RNA expression was quantified according to the Comparative C_T method described in User Bulletin #2 (Applied Biosystems, Foster City, CA, USA; updated 2001) relative to the housekeeping gene elongation factor 1-alpha (EF1-α). The relative changes in expression during ontogeny were determined by comparison to adult mRNA ΔC_T which was represented as 100%.

Data Analysis

Gene expression data are shown as mean ± standard error mean (SEM) of C_T values from a minimum of three animals per age group. Significance was determined by Student's t-test analysis at $p \leq 0.05$.

RESULTS

To identify morphological and developmental changes in protein and RNA expression patterns during nephrogenesis in the rhesus monkey, immunohistochemistry and quantitative

real-time PCR (qPCR) were utilized to analyze temporal and spatial expression of WT1, Pax2, Nestin, Synaptopodin, α-SMA, CD31, VEGF, and Gremlin.

Morphology

Kidney development in rhesus monkeys follows a pattern similar to humans as the intermediate mesoderm differentiates to form the mesonephros and the definitive metanephric kidney in the first trimester (Fig. 1A-E) (Matsell and Tarantal, 2002; Hiatt et al., 2010). The nephrogenic zone comprises roughly half of the developing tissue in the late first trimester and gradually decreases as gestation advances in human and nonhuman primates. Mature glomeruli and proximal and distal tubules were noted as early as the late first trimester in monkey kidneys (Fig. 1E) similar to humans (Saxen, 1987; Hiatt et al., 2010). With the development of the medullary region in the mid-second trimester, glomeruli begin maturation in the cortical region (Fig. 1F-K). Reciprocal inductive processes between the ureteric bud and the metanephric mesenchyme (blastema) triggers branching and elongation of the ureteric bud (future collecting system) and condensation and differentiation of the mesenchyme (future excretory component) (Saxen, 1987). The condensed mesenchyme was noted to form renal vesicles that differentiated into comma or C- and S-shaped bodies. With migration of the vascular endothelial component into the cleft of the S-shaped bodies, glomerular tuft formation begins and is followed by further differentiation of the distal tail of the S-shaped body into parietal epithelium of the glomerular capsule. The proximal epithelium of the S-shaped body then differentiates into a columnar structural entity forming podocyte precursors in the visceral epithelium of the glomerulus. Similar to humans, the nephrogenic zone disappears by the late third trimester in rhesus monkeys (Fig. 1M-N). In contrast to the mouse (Saxen, 1987), postnatal kidneys do not show evidence of nephrogenesis in human or nonhuman primates (Fig. 1O-Q; Fig. 2) (Matsell and Tarantal, 2002).

WT1

Early first trimester expression of WT1 was noted in the anterior-medial border of the neural crest, and in a region between the dorsal aorta and the mesonephros (Figs. 3A, 4A). Diffuse WT1 expression was observed in the metanephric mesenchyme, but not the ureteric bud, in the mid-first trimester (Fig. 3B). WT1 staining, while not apparent in the early renal vesicle, intensified as the renal vesicle differentiated into the C- and S-shaped bodies (Figs. 3C, 4C). In the second trimester, strong WT1 expression was noted in the tall columnar visceral epithelium of the developing glomerular tuft and the simple squamous parietal epithelium of the capsule (Figs. 3D-E, 4C-D) where it was co-expressed with Pax2 from the late-second trimester until Pax2 expression diminished in the mid-third trimester (Fig. 3F-G). Co-expression of WT1 with Nestin on glomerular tuft endothelium was noted in the second trimester (Fig. 4C-D). By the late third trimester and continuing into the postnatal period and adulthood, WT1 immunoreactivity was evident only in the podocytes of the glomerulus and in the arteriole endothelium (Fig. 3H-I) where it was co-expressed with Nestin (Fig. 4F-G).

Pax2

Pax2 was expressed in some cells of the mesonephros of the early first trimester embryo (Fig. 3A), and in the ureteric bud in mid-first trimester (Fig. 3B) where expression continued throughout the second trimester. Additional structures with Pax2 immunoreactivity in the late first trimester included the condensed mesenchyme surrounding the ureteric bud, the renal vesicle, and the developing C-shaped body (Fig. 3C). By the late second trimester, strong Pax2 staining was noted in the visceral and parietal epithelium (Fig. 3E) followed by Pax2 expression in the visceral epithelial layer of the glomerular tuft as podocyte differentiation proceeded (Fig. 3E-G). Postnatal expression of Pax2 was noted only in the parietal epithelial layer of the Bowman’s capsule near the vascular or urinary poles and in

isolated groups of cells just beneath the cortex, and in some, but not all, cells of the collecting ducts (Fig. 3H-I).

Nestin

Early first trimester expression of Nestin was noted in the neural crest (Figs. 4A, 5A) and in some cells in the mesonephros. The diffuse pattern of Nestin expression noted in the metanephric mesenchyme in the mid-first trimester largely disappeared by the end of the first trimester as Nestin expression was noted only in the induced blastema surrounding the ureteric bud tips (Figs. 4B, 5B). Although Nestin was not expressed in the renal vesicles, strong Nestin expression was noted in early glomerular tuft formation (Fig. 4C-E) and on the bordering surface of WT1-positive visceral epithelium of the glomerulus. Mature glomeruli located deep in the kidney cortex were noted with Nestin-positive cells, which were likely podocytes. With advancing gestational age, the location of Nestin-positive glomeruli expanded peripherally towards the outer cortex (Figs. 4F, 5C-F). From the mid-third trimester through early postnatal life, Nestin expression was noted solely on the glomerular podocytes (Fig. 4F-G) and vasculature including arcuate arteries and afferent arterioles (Fig. 4F-G). Podocyte co-expression of Nestin, WT1, and Synaptopodin was evident from the mid-third trimester to the adult (Figs. 4, 5F). The early visceral epithelial layer (developing podocytes) was noted with strong cytoplasmic expression of WT1 while Nestin expression was localized on the developing endothelium and/or the bordering surface of the visceral epithelium. As glomerular maturation progressed, Nestin expression was reduced in the glomerular endothelium but increased in the visceral epithelium of the glomerulus. By the late third trimester, Nestin was co-expressed with Synaptopodin in podocytes (Fig. 5F) although Synaptopodin immunoreactivity in maturing glomeruli was noted to be greater than Nestin immunoreactivity.

Synaptopodin

Some, but not all, of the tubule-shaped structures located below the metanephric zone of differentiation were immunoreactive for Synaptopodin in the late first trimester (Fig. 5A-B). The location and morphology of these Synaptopodin-positive structures suggests association with the ureteric bud. Synaptopodin staining was also noted in the region surrounding the notochord. In the early second trimester, limited Synaptopodin expression was observed on the membrane of visceral epithelial cells in contact with the glomerular capillary tuft (Fig. 5C-D). Co-expression with Nestin was noted at this stage of development. This pattern intensified with differentiation and, by the late third trimester, Synaptopodin expression was noted solely on podocytes (Fig. 5F).

Markers of Glomerular Development

Gremlin and α-SMA were included as markers in first and second trimester fetal kidneys to visualize early glomerular tuft development (Fig. 6A-B). In the late first trimester and into the second trimester Gremlin staining was observed on the luminal surface of the ureteric bud and developing glomerular tuft endothelium where it was co-expressed with CD31. High levels of Gremlin expression were noted in the early third trimester (Fig. 6C) in a pattern consistent with endothelial or mesangial cells, and was co-localized with CD31 on the luminal surface of developing glomerular endothelium. As expression of these markers was diminished in the third trimester, additional markers were studied including VEGF. Expression of α-SMA was observed in vascular smooth muscle (Fig. 6D) of arcuate arteries, afferent arterioles, and occasionally in developing glomerular endothelium although co-expression with VEGF was not noted (Fig. 6E).

Transcriptional Expression of Renal Developmental Markers

The transcriptional activity of key developmental genes was studied by quantitative RT-PCR analysis of expression patterns across gestation (Fig. 7). In general, patterns of transcript expression were similar to protein expression noted in the immunohistochemical analysis. Expression of WT1, Pax2, and α-SMA transcripts did not show any significant differences across gestation. In accordance with protein immunoreactivity described above, Nestin transcript expression declined 38% from the first to second trimesters (p=0.03) before increasing with podocyte maturation near term (relative copy number 8.8 in the second trimester compared with 17.5 at term; p=0.01). Likewise, Synaptopodin transcript expression was low in the first and second trimesters (1.0 and 0.7 relative copy numbers, respectively) before increasing with podocyte maturation in the third trimester (relative expression 2.2; p<0.05) and at term (relative expression 4.5; p<0.001). Expression of Gremlin mRNA increased more than two-fold from the first and second trimesters (16.1 and 21.5 relative copy numbers, respectively) to the third trimester (42.9 relative copy number; p<0.05) before declining sharply at term (relative expression 13.1; p<0.01).

Summary of Renal Markers by Structure and Gestational Age

A summary of expression of markers by structure and gestational age is provided in Table 2. Of the markers studied, Pax2 and Synaptopodin were expressed in the ureteric bud in the first trimester kidney with dim Gremlin expression noted at the branching tips. Pax2 was also expressed in the condensed mesenchyme surrounding the ureteric bud and in the early renal vesicle. WT1 and Nestin were diffusely expressed in the metanephric mesenchyme, but intensified as the Pax2-positive condensed mesenchyme differentiated into C- and S-shaped bodies. The inner cleft of the tail of the S-shaped body contained the podocyte progenitors (visceral epithelium) expressing Pax2, Nestin, and WT1 from the early second trimester. As kidney maturation progressed, Pax2 expression was lost in these structures and concurrent with an increase in Synaptopodin expression. Mature podocytes were observed from the mid-third trimester through adulthood, and expression of WT1, Nestin, and Synaptopodin was also shown. Early renal vasculature and glomerular endothelium were CD31, α-SMA, and Gremlin-positive. As the glomerular structures matured, Gremlin expression was restricted to mesangial cells and afferent arterioles in the mid-third trimester only. α-SMA immunoreactivity was noted in renal vascular smooth muscle postnatally and into adulthood (see Fig. 2).

DISCUSSION

This study represents the first detailed analysis of the protein and gene expression patterns for WT1, Pax2, Nestin, Synaptopodin, α-SMA, and Gremlin during renal ontogeny in the rhesus monkey. These data also indicate the timing of appearance of important nephrogenic structures (e.g., mesonephros, metanephric blastema, mesenchyme, renal vesicles, C- and S-shaped bodies, maturing nephrons), and highlight temporal similarities to humans which differ when compared to the mouse (Fig. 2) (Matsell and Tarantal, 2002). These studies provide a valuable reference for normal development in this species and for future translational studies of cell-based therapies for kidney repair (Tarantal et al., 2001; Butt et al., 2007; Batchelder et al., 2009; Leapley et al., 2009). In addition to localizing renal developmental markers to specific cell types, studies demonstrated that some markers (e.g., Pax2, WT1) continue to be expressed in the visceral epithelium of the glomerular tuft or the parietal epithelial layers of Bowman's capsule postnatally suggesting this location may be an important niche for less differentiated cells in the kidney. The first evidence of Gremlin immunoreactivity in developing mesangial cells was also shown during nephrogenesis in the rhesus monkey.

WT1 expression in the developing kidney of rhesus monkeys follows a pattern previously described in humans (Pritchard-Jones et al., 1990; Mundlos et al., 1993) and the mouse (Pelletier et al., 1991; Armstrong et al., 1992; Rackley et al., 1993; Georgas et al., 2008) with the strongest levels of expression observed in differentiating podocytes, in C- and S-shaped bodies, and in mature podocytes. These results show that cells that differentiate towards a podocyte lineage first express Pax2 (C- and S-shaped bodies), followed by strong WT1 expression as the visceral and parietal epithelial layers differentiate, and later by increased Nestin and Synaptopodin expression as podocyte maturation is completed. In agreement with the immunohistochemical analysis shown here and in previous reports in rodents (Sharma et al., 1992) and humans (Pritchard-Jones, et al., 1990), the greatest level of expression of WT1 was noted in podocytes in the third trimester, as terminal differentiation is completed. The gene expression data presented for WT1 suggest no changes in expression of this gene across gestation, but may be indicative of additional RNA regulation by small interfering RNAs (siRNAs) and microRNA's in some cell types (Perara, 2007; Agrawal et al., 2008; 2009).

The identification of renal multipotent progenitors has remained elusive and controversial, perhaps due in part to the complexity and variety of cell types found in the mature kidney. Fate-mapping experiments in mice have established that Osr1 expression in the intermediate mesoderm marks a nephrogenic progenitor population (Mugford et al., 2008) and that cap mesenchyme induced by the branching ureteric bud has populations of Six2 (Kobayashi et al., 2008) and Cited1 (Boyle et al., 2008) positive cells with self-renewal characteristics and multipotentiality. Stem cell markers CD24 and CD133 were studied in normal human fetal kidneys and localized to the renal vesicle and C- and S-shaped nephron (CD24) or the ureteric bud and uninduced metanephric blastema prior to induction (CD133) (Ivanova et al., 2010). In normal adult human kidney, these stem cell markers were co-expressed in cells of the macula densa. A population of CD24+CD133+ cells in embryeonic (Lazzeri et al., 2007) and adult (Sagrinati et al., 2006) human kidneys has also been identified, shown to restore renal function for induced acute renal failure in mice, and demonstrated to comprise hierarchical populations of progenitors in Bowman's capsule capable of regenerating tubules or podocytes depending on spatial location (Ronconi et al., 2009). Genetic tracing studies in mice demonstrated regeneration of podocytes from parietal epithelial cells (Appel et al., 2009). In accordance with these findings, the Pax2 and WT1 immunohistochemical analysis presented here demonstrates the persistence of these developmental markers in the parietal epithelium of Bowman's capsule in rhesus monkeys.

Studies to identify and characterize kidney progenitors for potential use for regenerative medicine will require surface markers to allow sorting of specific cell populations. Many of the nephrogenic progenitor markers identified, to date, are transcription factors such as Osr1, Six2, and Cited1 which limits the use of these markers for flow cytometric analysis. Similarly, the developmental markers included in this study are transcription factors with limited applications for sorting of the less-differentiated cell populations in fetal kidneys. Cell surface markers CD24 and CD133 have shown regenerative potential in human and mouse studies, but studies with these markers in nonhuman primates is limited because reactive antibodies are not currently available.

The spatial expression of Pax2 in early nephrogenic stages in the developing monkey kidney was similar to reports in human (Tellier et al., 2000) and mouse (Dressler et al., 1990) although the temporal development of the metanephric kidney begins earlier in human and nonhuman primates (first trimester) when compared to mouse (mid-gestation). The present study with rhesus monkey kidneys suggests expression of Pax2 follows a pattern in monkeys similar to humans with expression evident in the mesonephros and ureteric bud prior to condensation of induced mesenchyme in the late first trimester. The highest level of Pax2

expression was noted in the ureteric bud tips, the condensing mesenchyme, and the developing renal vesicle although expression was shown to be downregulated after the S-shaped body phase as noted in the mouse (Dressler and Douglass, 1992). Importantly, Pax2 appears to be downregulated in podocyte progenitors as WT1 expression increases (Ryan et al., 1995) as reported in the mouse suggesting regulatory control by WT1. Small, isolated groups of Pax2-positive cells remained in the outer cortex just under the kidney capsule until birth in mice (Dressler et al., 1990), and similar findings were noted in the early postnatal period in rhesus monkeys. Some cells of the parietal epithelium of Bowman's capsule continued to express Pax2 postnatally. These Pax2-positive cells, along with occasional cells expressing Pax2 in tubules in infants and adults, may represent a renal progenitor population with the potential to contribute to repair of glomeruli or tubules of the postnatal kidney.

This study has explored the expression of important renal developmental markers in rhesus monkeys across gestation, early postnatal life, and into adulthood. In parallel with quantitative RT-PCR, the spatial and temporal sequence of expression of these genes and localized expression to specific cell types and developmental structures has been identified. These studies form the basis for enhancing our understanding of nephrogenesis in the rhesus monkey, and will be important for translational studies where recapitulating early development will be necessary to repair kidneys damaged by congenital renal disease (Tarantal et al., 2001; Matsell et al., 2002; Butt et al., 2007).

Acknowledgments

The authors wish to thank the animal care staff at the California National Primate Research Center (CNPRC) for expert technical assistance, and Drs. Douglas Matsell and Mervin Yoder for review of the manuscript. These studies were supported by the National Institutes of Health (NIH) Center of Excellence in Translational Human Stem Cell Research (NIH grant #HL069748), the California Institute for Regenerative Medicine (CIRM) (#RC1-00144-1), the UC Davis Stem Cell Training Program (#T-00006), and the Primate Center base operating grant (#RR00169).

Grant sponsor: NIH; Grant numbers: HL069748, RR00169; Grant sponsor: The California Institute for Regenerative Medicine (CIRM); Grant number RC1-00144; and CIRM Training Grant number T1-00006.

LITERATURE CITED

Agrawal R, Tran U, Wessely O. Expression and functional analysis of miRNAs in kidney development. Dev Biol. 2008; 319:605. doi:10.1016/j.ydbio.2008.05.447.

Agrawal R, Tran U, Wessely O. The miR-30 miRNA family regulates *Xenopus* pronephros development and targets the transcription factor Xlim1/Lhx1. Development. 2009; 136:3927–3936. [PubMed: 19906860]

Appel D, Kershaw DB, Smeets B, Yan G, Fuss A, Frye B, Elger M, Kriz W, Floege J, Moeller MJ. Recruitment of podocytes from glomerular parietal epithelial cells. J Am Soc Nephrol. 2009; 20:333–343. [PubMed: 19092119]

Armstrong JF, Pritchard-Jones K, Bickmore WA, Hastie ND, Bard JBL. The expression of the Wilms' tumour gene, WT1, in the developing mammalian embryo. Mech Dev. 1992; 40:85–97. [PubMed: 8382938]

Batchelder CA, Lee CCI, Matsell DG, Yoder MC, Tarantal AF. Renal ontogeny in the rhesus monkey (*Macaca mulatta)* and directed differentiation of human embryonic stem cells towards kidney precursors. Differentiation. 2009; 78:45–56. [PubMed: 19500897]

Barisoni L, Mokrzycki M, Sablay L, Nagata M, Yamase H, Mundel P. Podocyte cell cycle regulation and proliferation in collapsing glomerulopathies. Kidney Int. 2000; 58:137–143. [PubMed: 10886558]

Bertelli E, Regloi M, Fonzi L, Occhini R, Mannucci S, Ermini L, Toti P. Nestin expression in adult and developing human kidney. J Histochem Cytochem. 2007; 55:411–421. [PubMed: 17210924]

Bontrop RE. Non-human primates: Essential partners in biomedical research. Immunol Rev. 2001; 183:5–9. [PubMed: 11782243]

Boyle S, Misfeldt A, Chandler KJ, Deal KK, Southard-Smith EM, Mortlock DP, Baldwin HS, de Caestecker M. Fate mapping using *Cited1-CreER*^{T2} mice demonstrates that the cap mesenchyme contains self-renewing progenitor cells and gives rise exclusively to nephronic epithelia. Dev Biol. 2008; 313:234–245. [PubMed: 18061157]

Butt MJ, Tarantal AF, Jimenez DF, Matsell DG. Collecting duct epithelial-mesenchymal transition in fetal urinary tract obstruction. Kidney Int. 2007; 72:936–944. [PubMed: 17667982]

Charles AK, Mall S, Watson J, Berry PJ. Expression of the Wilms' tumour gene WT1 in the developing human and in paediatric renal tumours: an immunohistochemical study. J Clin Pathol: Mol Pathol. 1997; 50:138–144.

Chen J, Boyle S, Zhao, Su W, Takahashi K, Davis L, DeCaestecker M, Takahashi T, Breyer MD, Haeo C-M. Differential expression of the intermediate filament protein nestin during renal development and its localization in adult podocytes. J Am Soc Nephrol. 2006; 17:1283–1291. [PubMed: 16571784]

Coresh J, Selvin E, Stevens LA, Manzi J, Kusek JW, Eggers P, Van Lente F, Levey AS. Prevalence of chronic kidney disease in the United States. JAMA. 2007; 298:2038–2047. [PubMed: 17986697]

Dressler GR, Deutsch U, Chowdhury K, Nornes HO, Gruss P. Pax2, a new murine paired-box containing gene and its expression in the developing excretory system. Development. 1990; 109:787–795. [PubMed: 1977574]

Dressler GR, Douglass EC. Pax-2 is a DNA-binding protein expressed in embryonic kidney and Wilms' tumor. Proc Natl Acad Sci USA. 1992; 89:1179–1183. [PubMed: 1311084]

Georgas K, Rumballe B, Wilkinson L, Chiu HS, Lesieur E, Gilbert T, Little MH. Use of dual section mRNA *in situ* hybridization/immunohistochemistry to clarify gene expression patterns during the early stages of nephron development in the embryo and in the mature nephron of the adult mouse kidney. Histochem Cell Biol. 2008; 130:927–942. [PubMed: 18618131]

Hiatt MJ, Ivanova L, Toran N, Tarantal AF, Matsell DG. Remodeling of the fetal collecting duct epithelium. Am J Pathol. 2010; 176:630–637. [PubMed: 20035053]

Ivanova L, Hiatt MJ, Yoder MC, Tarantal AF, Matsell DG. Ontogeny of CD24 in the human kidney. Kidney Int. Mar 24.2010 [Epub ahead of print].

Kobayashi A, Valerius MT, Mugford JW, Carroll TJ, Self M, Oliver G, McMahon AP. Six2 defines and regulates a multipotent self-renewing nephron progenitor population throughout mammalian kidney development. Cell Stem Cell. 2008; 3:169–181. [PubMed: 18682239]

Lazzeri E, Crescioli C, Ronconi E, Mazzinghi B, Sagrinati C, Netti GS, Angelotti ML, Parente E, Ballerini L, Cosmi L, Maggi L, Gesualdo L, Rotondi M, Annunziato F, Maggi E, Lasagni L, Serio M, Romagnani S, Vannelli GB, Romagnani P. Regenerative potential of embryonic renal multipotent progenitors in acute renal failure. J Am Soc Nephrol. 2007; 18:3128–3138. [PubMed: 17978305]

Leapley AC, Lee CC, Batchelder CA, Yoder MC, Matsell DG, Tarantal AF. Characterization and culture of fetal rhesus monkey renal cortical cells. Pediatr Res. 2009; 66:448–54. [PubMed: 19581826]

Lee CI, Goldstein O, Han VKM, Tarantal AF. IGF-II and IGF binding protein (IGFBP-1, IGFBP-3) gene expression in fetal rhesus monkey tissues during the second and third trimesters. Pediatr Res. 2001; 49:379–387. [PubMed: 11228264]

Little MH, Rae FK. Potential cellular therapies for renal disease: Can we translate results from animal studies to the human condition? Nephrology. 2009; 14:544–553. [PubMed: 19712255]

MacPherson BR, Leslie KO, Lizaso KV, Schwarz JE. Contractile cells of the kidney in primary glomerular disorders: An immunohistochemical study using an anti-alpha-smooth muscle actin monoclonal antibody. Hum Pathol. 1993; 24:710–716. [PubMed: 8319951]

Matsell DG, Mok A, Tarantal AF. Altered primate glomerular development due to *in utero* urinary tract obstruction. Kidney Int. 2002; 61:1263–1269. [PubMed: 11918732]

Matsell DG, Tarantal AF. Experimental models of fetal obstructive nephropathy. Pediatr Nephrol. 2002; 17:470–476. [PubMed: 12172756]

McMahon R, Murphy M, Clarkson M, Taal M, Mackenzie HS, Godson C, Martin F, Brady HR. *IHG-2*, a mesangial cell gene induced by high glucose, is human *gremlin*. J Biol Chem. 2000; 275:9901–9904. [PubMed: 10744662]

Mezquita P, Beard BC, Kiem HP. NOD/SCID repopulating cells contribute only to short-term repopulation in the baboon. Gene Ther. 2008; 15:1460–1462. [PubMed: 18563183]

Mundel P, Gilbert P, Kriz W. Podocytes in glomerulus of rat kidney express a characteristic 44 kd protein. J Histochem Cytochem. 1991; 39:1047–1056. [PubMed: 1856454]

Mundel P, Heid HW, Mundel TM, Krüger M, Reiser J, Kriz W. Synaptopodin: An actin-associated protein in telencephalic dendrites and renal podocytes. J Cell Biol. 1997; 139:193–204. [PubMed: 9314539]

Mundlos S, Pelletier J, Darveau A, Bachmann M, Winterpacht A, Zabel B. Nuclear localization of the protein encoded by the Wilms' tumor gene WT1 in embryonic and adult tissues. Development. 1993; 119:132901341.

Mugford JW, Sipilä P, McMahon JA, McMahon AP. Osr1 expression demarcates a multipotent population of intermediate mesoderm that undergoes progressive restriction to an Osr1-dependent nephron progenitor compartment within the mammalian kidney. Dev Biol. 2008; 324:88–98. [PubMed: 18835385]

Nagata M, Nakayama K, Terada Y, Hoshi S, Watanabe T. Cell cycle regulation and differentiation in the human podocyte lineage. Am J Pathol. 1998; 153:1511–1520. [PubMed: 9811343]

Naruse K, Fujieda M, Miyazaki E, Hayashi Y, Toi M, Fukui T, Kuroda N, Hiroi M, Kurashige T, Enzan H. An immunohistochemical study of developing glomeruli in human fetal kidneys. Kidney Int. 2000; 57:1836–1846. [PubMed: 10792602]

Nirmalanandhan VS, Sittampalam GS. Stem cells in drug discover, tissue engineering, and regenerative medicine: Emerging opportunities and challenges. J Biomolec Screen. 2009; 14:755–768.

Organ Procurement and Transplantation Network. Current US Waiting List by Organ, US DHHS. 2008. http://optn.transplant.hrsa.gov/latestData/rptData.asp

Pelletier J, Schalling M, Buckler AJ, Rogers A, Haber DA, Housman D. Expression of the Wilms' tumor gene WT1 in the murine urogenital system. Genes Dev. 1991; 5:1345–1356. [PubMed: 1651275]

Pritchard-Jones K, Fleming S, Davidson D, Bickmore W, Porteous D, Gosden C, Bard J, Buckler A, Pelletier J, Housman D, van Heyningen V, Hastie N. The candidate Wilms' tumour gene is involved in genitourinary development. Nature. 1990; 346:194–197. [PubMed: 2164159]

Rackley RR, Flenniken AM, Kuriyan NP, Kessler PM, Stoler MH, Williams BRG. Expression of the Wilms' Tumor suppressor gene WT1 during mouse embryogenesis. Cell Growth Diff. 1993; 4:1023–1031. [PubMed: 8117616]

Rao PK, Palmer JS. Prenatal and postnatal management of hydronephrosis. Sci World J. 2009; 13:606–614.

Ronconi E, Sagrinati C, Angelotti ML, Lazzeri E, Mazzinghi B, Ballerini L, Parente E, Becherucci F, Gacci M, Carini M, Maggi E, Serio M, Vannelli GB, Lasagni L, Romagnani S, Romangnani P. Regeneration of glomerular podocytes by human renal progenitors. J Am Soc Nephrol. 2009; 20:322–332. [PubMed: 19092120]

Ryan G, Steele-Perkins V, Morris JF, Rauscher FJ, Dressler GR. Repression of Pax-2 by WT1 during normal kidney development. Development. 1995; 121:867–875. [PubMed: 7720589]

Sagrinati C, Netti GS, Mazzinghi B, Lazzeri E, Liotta F, Frosali F, Ronconi E, Meini C, Gacci M, Squecco R, Carini M, Gesualdo L, Francini F, Maggi E, Annunziato F, Lasagni L, Serio M, Romagnani S, Romagnani P. Isolation and characterization of multipotent progenitor cells from Bowman's capsule of adult human kidneys. J Am Soc Nephrol. 2006; 17:2443–2456. [PubMed: 16885410]

Saxen, L. Organogenesis of the kidney. In: Barlow, PW.; Green, PB.; White, CC., editors. Developmental and Cell Biology Series. Vol. Vol. 19. Cambridge University Press; Cambridge, UK: 1987. p. 1-171.

Sharma PM, Yang X, Bowman M, Roberts V, Sukumar S. Molecular cloning of rat Wilms' Tumor complementary DNA and a study of messenger RNA expression in the urogenital system and the brain. Cancer Res. 1992; 52:6407–6412. [PubMed: 1330293]

Shively CA, Clarkson TB. The unique value of primate models in translational research. Am J Primatol. 2009; 72:715–721. [PubMed: 19507247]

Perara RJ. A microarray-based method to profile global microRNA expression in human and mouse. Methods Mol Biol. 2007; 382:137–148. [PubMed: 18220229]

Tarantal, AF. Ultrasound imaging in rhesus (*Macaca mulatta*) and long-tailed (*Macaca fascicularis*) macaques: Reproductive and research applications. In: Wolfe-Coote, S., editor. The Laboratory Primate. Elsevier; Amsterdam: 2005. p. 317-351.

Tarantal AF, Han VK, Cochrum KC, Mok A, daSilva M, Matsell DG. Fetal rhesus monkey model of obstructive renal dysplasia. Kidney Int. 2001; 59:446–456. [PubMed: 11168926]

Tellier A-L, Amiel J, Delezoide A-L, Audollent S, Augé J, Esnault D, Encha-Razavi F, Munnich A, Lyonnet S, Vekemans M, Attié-Bitach T. Expression of the PAX2 gene in human embryos and exclusion in the CHARGE syndrome. Am J Med Genet. 2000; 93:85–88. [PubMed: 10869107]

Wagner N, Wagner K-D, Scholz H, Kirschner KM, Schedl A. Intermediate filament protein nestin is expressed in developing kidney and heart and might be regulated by the Wilms' tumor suppressor Wt1. Am J Physiol Reg Integr Comp Physiol. 2006; 291:779–787.

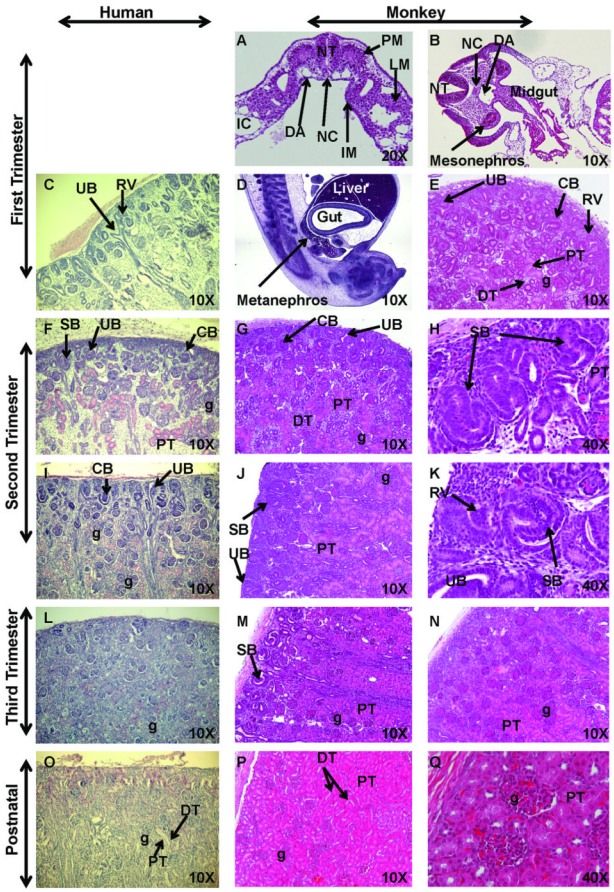

Figure 1. Hematoxylin and Eosin (H&E) staining of sequential stages of kidney development

Sections of first trimester rhesus monkey embryos highlight development of the intermediate mesoderm (IM) (Fig. 1A; early first trimester transverse section), mesonephros (Fig. 1B; mid-first trimester transverse section), and definitive kidney or metanephros (Fig. 1D, sagittal section, and 1E; late first trimester). These developmental findings for nephrogenic structures were similar when compared to human fetal kidneys (8 weeks) (Fig. 1C) (courtesy of Dr. Douglas Matsell; collected in accordance with the Human Ethics Guidelines of the University of British Columbia). Second trimester images illustrate active nephrogenesis in the outer cortex in both human (Fig. 1F, I; 18 and 26 weeks, respectively; courtesy of D. Matsell) and monkey (Fig. 1G-H; early second trimester and Fig. 1J-K; mid-second trimester). Third trimester fetal kidney sections demonstrated nephrogenesis is nearing completion with restriction of the nephrogenic zone in human (Fig. 1L; 36 weeks; courtesy of D. Matsell) and monkey (Fig. 1M-N; mid-third trimester). Postnatal human (Fig. 1O; 5 years; courtesy of D. Matsell) and monkey kidneys (Fig. 1P-Q; 6 months) are shown. Abbreviations: CB, C-shaped body; DA, dorsal aorta; DT, distal tubule; IC, intraembryonic coelom; g, glomerulus; LM, lateral mesoderm; PM, paraxial mesoderm; NC, notochord; NT, neural tube; PT, proximal tubule; RV, renal vesicle; SB, S-shaped body; UB, ureteric bud.

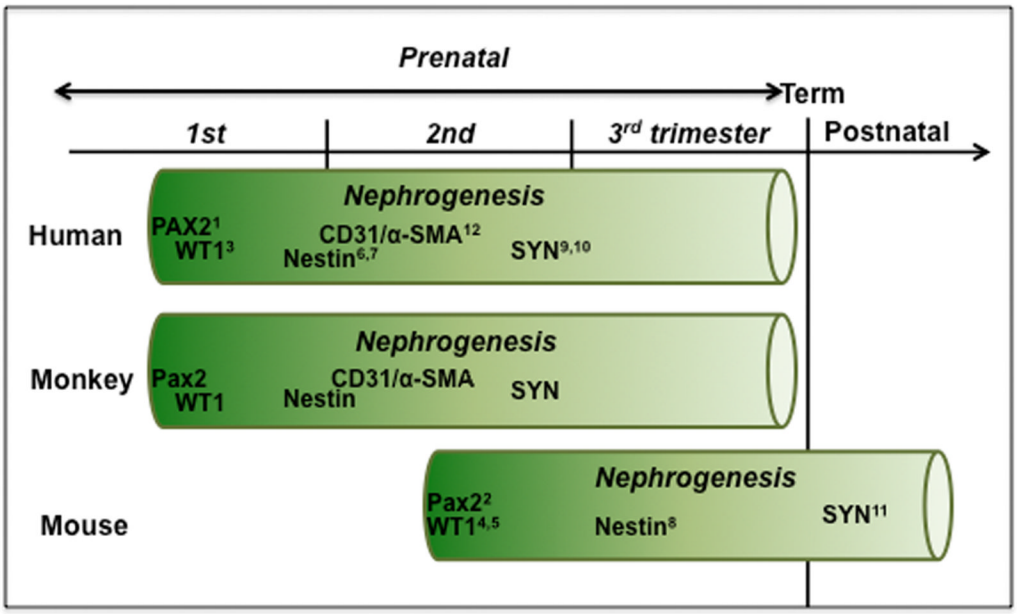

Figure 2. Time course of nephrogenesis and expression of renal developmental markers in human, monkey, and mouse

Nephrogenesis begins in human and nonhuman primates in the late first trimester and continues throughout the mid-third trimester (term 165±10 days). In contrast, mouse nephrogenesis begins in mid-gestation and concludes postnatally (Saxen, 1987) (term 20 days). ([1]Tellier et al., 2000; [2]Dressler et al., 1990; [3]Charles et al., 1997; [4]Armstrong et al., 1992; [5]Rackley et al., 1993; [6]Bertelli et al., 2007; [7]Wagner et al., 2006; [8]Chen et al., 2006, [9]Nagata et al., 1998; [10]Barisoni et al., 2000; [11]Mundel et al., 1991; [12]Naruse et al., 2000).

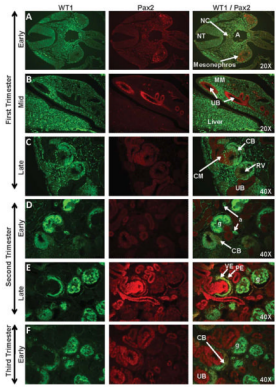

Figure 3. WT1 and Pax2 staining of sequential stages of kidney development in rhesus monkeys

Pax2 expression was noted from the early first trimester through the late third trimester in the mesonephros (Fig. 3A), ureteric bud (UB) (Fig. 3B), condensed mesenchyme (CM) (Fig. 3C-H), and renal vesicle (RV) (Fig. 3C) of the nephrogenic zone. Isolated collecting duct (CD) cells (Fig. 3I) continued to express Pax2 postnatally; this marker was also noted in widely scattered pockets of cells under the cortical capsule (Fig. 3I-J; 3-6 months postnatal WT1/Pax2 composite images). WT1 was expressed in the genital ridge between the aorta (A) and the mesonephros (Fig. 3A) and in the metanephric mesenchyme (MM) (Fig. 3B) in the mid-first trimester, followed by the C- and S-shaped bodies (CB and SB, respectively) (Fig. 3C-G), arterioles (a), and the visceral epithelium (VE) of the glomerulus where it was co-expressed with Pax2. The parietal epithelial layer (PE) did not express WT1 but showed isolated Pax2-positive cells that were closely associated with the vascular or urinary pole of the glomerulus (g) (Fig. 3E-G). Images oriented with the cortex to the upper left (Fig. 3C-K). NT, neural tube; NC, notochord; PT, proximal tubule.

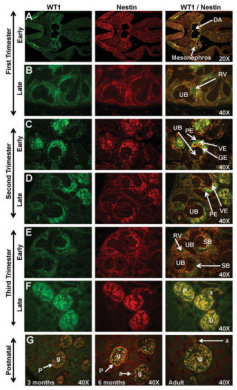

Figure 4. WT1 and Nestin expression in sequential stages of kidney development in rhesus monkeys

In the early first trimester, WT1 was localized between the dorsal aorta (DA) and the mesonephros (Fig. 4A) while Nestin was expressed in the mesonephros. Dim expression of these markers was noted in the mid to late-first trimester metanephric kidney (Fig. 4B). Neither marker was expressed in the ureteric bud (UB). Faint WT1 expression was noted as the renal vesicle (RV) differentiated in the tail of the comma or C-shaped body. In the second trimester (Fig. 4C-D) and early third trimester (Fig. 4F), WT1 was strongly expressed on the visceral epithelium (VE) of the glomerulus with Nestin expression noted surrounding the developing glomerular endothelium (GE). The parietal epithelium (PE) of Bowman's capsule was negative for both markers. By the mid-third trimester and continuing postnatally (Fig. 4F-G), these markers were expressed in the podocytes (P) of the glomeruli (g) and the afferent arterioles (a). Images oriented with cortex to the upper left. SB, S-shaped body. Postnatal (Fig. 4G) images are presented as a composite of WT1/Nestin.

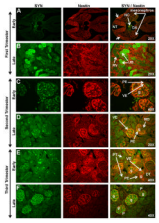

Figure 5. Synaptopodin (SYN) and Nestin expression in sequential stages of kidney development in rhesus monkeys

In the early first trimester, Synaptopodin expression was noted in the notochord (NC) and surrounding region between the dorsal aorta (DA) and the neural tube (NT) (Fig. 5A). Nestin was localized to the mesonephros and the neural crest (arrows). Synaptopodin expression was observed in the ureteric bud (UB) in the late first trimester (Fig. 5B). Early second trimester expression of these markers was found in the visceral epithelial layer (VE) of mature glomeruli (g) deep in the medulla (Fig. 5C). Both markers were absent in the parietal epithelium (PE) of Bowman's capsule. Synaptopodin expression in the outer cortical region was noted in late second trimester (Fig. 5D) on developing podocytes. This staining pattern intensified throughout the third trimester (Fig. 5E-F) where Synaptopodin and Nestin were co-expressed on podocytes (P). Images oriented with cortex to upper left. DT, distal tubule; MD, macula densa; RV, renal vesicle.

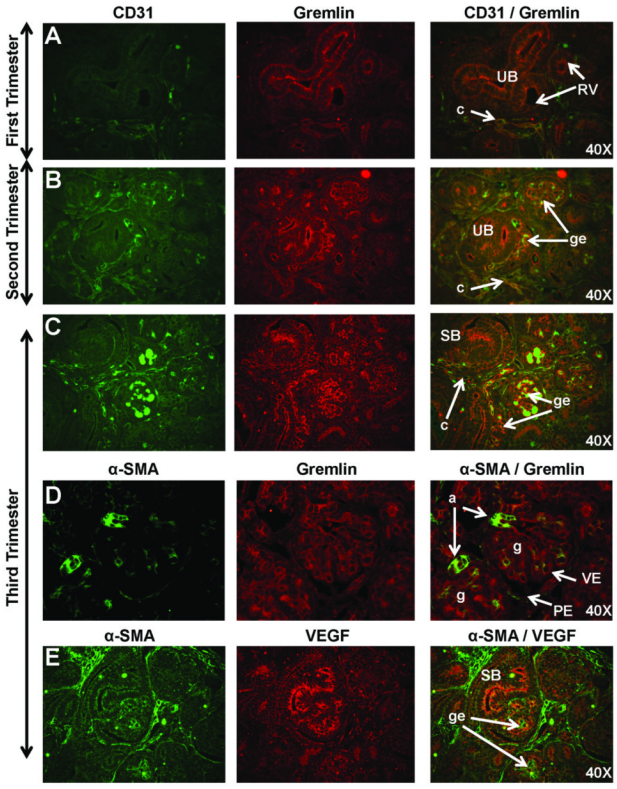

Figure 6. Markers of glomerular tuft development including CD31, Gremlin, alpha-smooth muscle actin (α-SMA), and vascular endothelial growth factor (VEGF) in sequential stages of nephrogenesis in rhesus monkeys

Dim CD31 immunoreactivity was observed on capillaries (c) in the metanephric blastema (Fig. 6A) while Gremlin staining was observed on the luminal surface of the ureteric bud (UB). Gremlin staining was stronger on the developing glomerular endothelium (ge) where it was co-expressed with CD31 in the second (Fig. 6B) and early third trimesters (Fig. 6C). By the mid-third trimester, only dim Gremlin expression was observed in a pattern consistent with endothelial or mesangial cells, and on the luminal surface of α-SMA-positive vasculature (Fig. 6D). Bright α-SMA expression was noted in vascular smooth muscle of arcuate arteries (not shown) and afferent arterioles (a). In the mid-second trimester, dim VEGF staining was noted followed by bright VEGF expression in third trimester glomerular endothelium (Fig. 6E). Images oriented with the cortex to upper left. PE, parietal epithelium; RV, renal vesicle; SB, S-shaped body; VE, visceral epithelium.

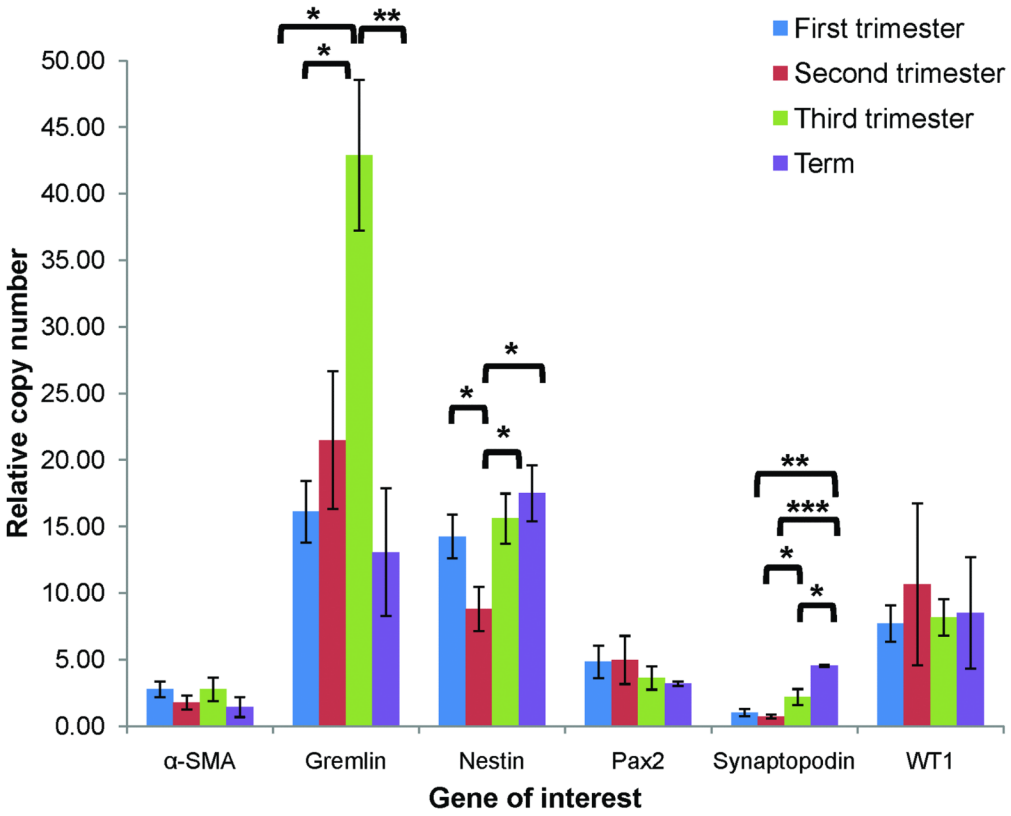

Figure 7. Quantitative RT-PCR analysis of expression patterns of α-SMA, Gremlin, Nestin, Pax2, Synaptopodin, and WT1 across gestation

RNA expression was quantified according to the comparative C_T method with EF1-α as the housekeeping gene and relative changes in expression determined by comparison to adult mRNA taken as 100% (see text); *p<0.05, **p<0.01, ***p<0.001. An N≥3 was included for each age group.

Table 1

Primer sequences for renal developmental markers

Gene	Primer	Sequence
WT1	Forward Primer Reverse Primer	5′-CTTCAGAGGCATTCAGGATGTG-3′ 5′-TCTCAGATGCCGACCGTACA-3′
Pax2	Forward Primer Reverse Primer	5′-GCTTTGGATCGGGTCTTTGA -3′ 5′-CTCGTTCCCCTGTTCTGATTTG-3′
Nestin	Forward Primer Reverse Primer	5′-TGGCAAGAGGCCGGTACA-3′ 5′-CCGTATTTGTCCTTCACCTTC-3′
Synaptopodin	Forward Primer Reverse Primer	5′-CAGATTGGGCCAGAGCACTAG-3′ 5′-TTGGACGCCACGGGAAT-3′
α-SMA	Forward Primer Reverse Primer	5′-GGGACGACATGGAAAAGATCTG-3′ 5′-GCAGGGTGGGATGCTCTTC-3′
Gremlin	Forward Primer Reverse Primer	5′-ATGTGACCGAGCGCAAATAC-3′ 5′-TGGATATGCAACGACACTGC-3′
EF1-α	Forward Primer Reverse Primer	5′-GACCCACCAATGGAAGCAG-3′ 5′-TGTGGCAATCCAATACAGGG-3′

WT1=Wilm’s tumor 1; Pax2=paired box 2; α-SMA; α-SMA=alpha-smooth muscle actin; EF1-α=housekeeping gene elongation factor 1-alpha

Table 2

Summary of distribution of renal developmental markers in fetal rhesus monkeys

	MM	UB	CM	Renal vesicle	C-shaped	S-shaped	Prenatal glomerulus	Postnatal glomerulus	CD	V
WT1	++	−	−	−	++	+	++VE, +++P	++P	−	+AA
Pax2	−	++	++	+++	+	+	+PE,+VE	+/−PE, +/− VE	+/−	−
Nestin	++	−	−	−	−	+	++P	+P	−	+AA
Synaptopodin	−	+/−	−	−	−	+	++P	+P	−	−
α-SMA	+	−	−	−	−	+	+/−EN, +M	−	−	+SM
Gremlin	−	+/−	−	−	−	+	+EN, +M	−	−	−

WT1=Wilm's tumor 1; Pax2=paired box 2; α-SMA=alpha-smooth muscle actin.

MM=metanephric mesenchyme; UB=ureteric bud; CM=condensed mesenchyme; CD, collecting duct; V, vasculature excluding glomerular endothelium.

VE=visceral epithelium; PE=parietal epithelium; P=podocytes; AA=afferent arterioles; EN=glomerular endothelium; M=mesangial cells; SM=vascular smooth muscle.

Qualitative expression of each marker represented by + (dim expression), ++ (moderate expression), +++ (strong expression), +/− (variable expression), − (no expression).

Anat Rec (Hoboken). Author manuscript; available in PMC 2011 November 1.